

## Improving aeroelastic characteristics of helicopter rotor blades in hovering

Hossam T. Badran<sup>\*1,3</sup>, Mohammad Tawfik<sup>2a</sup> and Hani M. Negm<sup>3b</sup>

<sup>1</sup>Arab Organization for Industrialization, Cairo 11421, Egypt

<sup>2</sup>Academy of Knowledge, Cairo 11765, Egypt

<sup>3</sup>Aerospace Engineering Department, Cairo University, Giza 12613, Egypt

(Received February 8, 2021, Revised May 2, 2021, Accepted May 17, 2021)

**Abstract.** Flutter is a dangerous phenomenon encountered in flexible structures subjected to aerodynamic forces. This includes aircraft, helicopter blades, engine rotors, buildings and bridges. Flutter occurs as a result of interactions between aerodynamic, stiffness, and inertia forces on a structure. The conventional method for designing a rotor blade to be free from flutter instability throughout the helicopter's flight regime is to design the blade so that the aerodynamic center (AC), elastic axis (EA) and center of gravity (CG) are coincident and located at the quarter-chord. While this assures freedom from flutter, it adds constraints on rotor blade design which are not usually followed in fixed wing design. Periodic Structures have been in the focus of research for their useful characteristics and ability to attenuate vibration in frequency bands called "stop-bands". A periodic structure consists of cells which differ in material or geometry. As vibration waves travel along the structure and face the cell boundaries, some waves pass and some are reflected back, which may cause destructive interference with the succeeding waves. In this work, we analyze the flutter characteristics of helicopter blades with a periodic change in their sandwich material using a finite element structural model. Results shows great improvements in the flutter rotation speed of the rotating blade obtained by using periodic design and increasing the number of periodic cells.

**Keywords:** aeroelastic; finite element; flutter; helicopter; hovering; periodic structure; rotor, vibration

### 1. Introduction

Carrera Unified Formulation (CUF) is used to perform flutter analyses of fixed and rotary wings. The finite element method is used to solve the governing equations that are derived, in a weak form, using the generalized Hamilton's Principle. These equations are written in terms of CUF "fundamental nuclei", which do not vary with the theory order (N) Filippi and Carrera (2015). An aeroelastic analysis of bearingless rotors is investigated using large deflection beam theory in hover and forward flight. The sectional elastic constants of a composite flex beam, including the warping deformations, are determined from a refined cross-sectional finite element method Lim and Lee (2009). A new finite element model based on the coupled displacement field and the tapering functions of the beam is formulated for transverse vibrations of rotating

---

\*Corresponding author, Ph.D., E-mail: htbadran@hotmail.com, htbadran@gmail.com

<sup>a</sup>Associate Professor, E-mail: mohammad.tawfik@gmail.com

<sup>b</sup>Professor, E-mail : hnegm\_cu@hotmail.com

Timoshenko beams of equal strength Yardimoglu (2010). Kee and Shin (2015) investigate the dynamic characteristics of rotating composite blades. An eighteen-node solid-shell finite element was used to model the blade structures. The equations of motion for the finite element model were derived by using Hamilton's principle, and the resulting nonlinear equilibrium equations were solved by applying Newton-Raphson method combined with load control. A rotating beam finite element in which the interpolating shape functions are obtained by satisfying the governing static homogenous differential equation of Euler–Bernoulli rotating beams is developed by Babu Gunda and Ganguli (2008).

Loewy's 2-D unsteady aerodynamic theory Loewy (1957), as amended by Jones and Rao (1970) and Hammond (1969), provides a useful tool for examining blade flutter in hover. Additionally, Loewy showed how shed layers of vorticity affect Theodorsen's lift deficiency function Theodorsen (1935), and influence the unsteady aerodynamic lift and moment equations. The present work will follow the analysis of Shipman and Wood, using Theodorsen's lift deficiency function. Carleton University's Rotorcraft Research Group is working on the development of an active rotor control system that incorporates a mechanism for helicopter blade pitch dynamic stiffness modulation at the root, the Active Pitch Link. Flutter oscillations of a typical section were controlled out over a range of airflow speeds (Nitzsche *et al.* 2015). (Badran *et al.* 2019) analyze the flutter characteristics of helicopter blades with a periodic change in their sandwich material using a finite element structural model. Results shows great improvements in the flutter forward speed of the rotating blade obtained by using periodic design and increasing the number of periodic cells. (Dayhoum *et al.* 2020) provide an improvement for rotating wings in forward flight by adding experimental elastic torsion as an input to the local angle of attack.

## 2. Periodic structures

A periodic structure consists fundamentally of a number of identical substructure components that are joined together to form a continuous structure. Recall what happens to Light wave as it travels through a boundary between two different media; part of the light wave refracts inside the water and the another part reflects back into air. The mechanical waves behave in a similar way and the reflected part of wave interferes with the incident wave, Mead (1996).

There are two main types of discontinuities: (1) Geometric discontinuity and (2) Material discontinuity. Fig. 1 shows the basic idea of periodic structures and two different types of discontinuities. The transfer matrix approach, in general, is based on developing a relation between the two ends of a structural element. The real power of the transfer matrix approach comes when the structure can be divided into a set of substructures with a set of elements and nodes that are connected to another set on some fictitious boundary inside the structure, Mead and Parthan (1979).

Using the method of static condensation, the internal nodes/degrees of freedom of the substructure can be eliminated, thus reducing the size of the global matrices of the structure. When the set of equations of the substructure can be manipulated to collect the forces and displacements of one end of the substructure on one side of the equation, and relate them to those on the other end with a matrix relation, this matrix relation is called the transfer matrix of the structure. The transfer matrix of a substructure, other than being of reduced order, is then multiplied by that of the neighboring structure, in contrast with the superposition method that is used in conventional numerical techniques. Thus, the matrix system that describes the dynamics of the structure

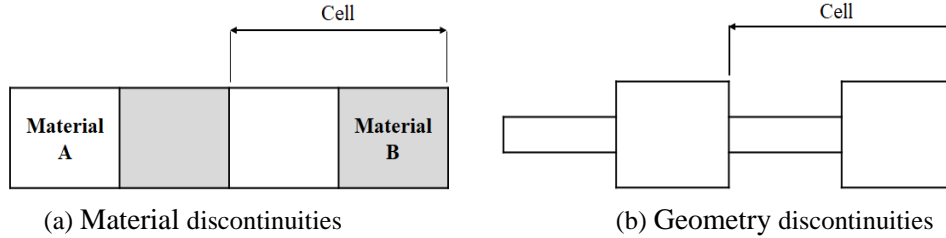


Fig. 1 Type of discontinuities

becomes of significantly smaller size. The transfer matrix method becomes of even more appealing features when the substructures can be selected in a manner that they are all identical, thus, calculating the transfer matrix for one substructure is sufficient to describe the dynamics of the whole structure easily. An efficient numerical approach is proposed to study free and forced vibration of complex one-dimensional (1D) periodic structures (Zhou *et al.* 2015).

### 3. Mathematical modelling

A sandwiched rotating blade consists of 3 layers; a ceramic with rigid foam sandwiched between two aluminum layers. All layers are supposed to be perfectly bonded, under in plane-stress state, and having the same transverse displacement. The deformation of the face sheets obeys Euler-Bernoulli theory, while that of the core obeys Timoshenko theory. We will define all the mechanical quantities such as displacements, strains and energies in terms of the transverse displacements ( $w$ ) and longitudinal displacements of the top and bottom layers ( $u_t$ ) and ( $u_b$ ), respectively as shown in (Badran *et al.* 2017). The longitudinal displacements of the layers are linear, the top and bottom layers resist axial and bending loads only, and the core layer resists shear load in addition to axial and bending loads. All layers resist torsion and centrifugal loads.

### 4. Development of equations of motion

The dynamic equations of motion in this investigation are developed using Hamilton's principle, Reddy (2002):

$$\delta \Pi = \int_{t_1}^{t_2} (\delta T - \delta U + \delta W) dt = 0 \tag{1}$$

By introducing and taking the first variation for strain energy, kinetic energy and external work, then integrating by parts with respect to time ( $t_1$  and  $t_2$  are arbitrary) we get the weak form of Hamilton's principle, which is used for deriving the finite element equations of the system. Since all layers bear axial, bending, torsion loads, and the core bears, in addition shear loads, then the total strain energy of the proposed model can be cast in this form:

$$U_i = \frac{1}{2} E^i A^i \int_0^L (u_i')^2 dx + \frac{1}{2} E^i I^i \int_0^L (w'')^2 dx + \frac{1}{2} G^i J^i \int_0^L (\varphi')^2 dx \tag{2}$$

$$U_c = \frac{1}{2} E^c A^c \int_0^L (u_c')^2 dx + \frac{1}{2} E^c I^c \int_0^L (\theta')^2 dx + \frac{1}{2} K_s G^c A^c \int_0^L (\gamma_{xz})^2 dx + \frac{1}{2} G^c J^c \int_0^L (\varphi')^2 dx \quad (3)$$

The bending and torsion strain energy due to rotation is given by,

$$U_R = \frac{1}{2} (\rho^j A^j) \int_0^L f_c(x) (w')^2 dx + \frac{1}{2} (\rho^j I_o^j) \int_0^L f_c(x) (\varphi')^2 dx \quad (4)$$

The total kinetic energy for the proposed model can be cast in this form:

$$T_i = \frac{1}{2} \rho_i \int_0^L [A_i (\dot{u}_i)^2 + I_i (\dot{w}')^2 + A_i (\dot{w})^2] dx \quad (5)$$

$$T_c^p = \frac{1}{2} \rho_c \int_0^L [A_c (\dot{u}_c)^2 + I_c (\dot{\theta}_c)^2 + A_c (\dot{w})^2] dx \quad (6)$$

The external work applies on the proposed model is,

$$W_t = \int_V \{q\}^T \{f_b\} dV + \int_A \{q\}^T \{f_s\} dA + \{q\}^T \{f_p\} \quad (7)$$

where:  $\{f_b\}$ ,  $\{f_s\}$  and  $\{f_p\}$  and  $\{q\}$  are the external body, surface , point forces, and nodal displacements respectively.

#### 4.1 Introducing centrifugal force $f_c(x)$

As shown in Fig. 2, the centrifugal force induced by rotation at station (x) within the  $i^{th}$  element, measured from its left end can be expressed as mentioned in (Badran *et al.* 2019):

$$f_c(x) = \Omega^2 \int_x^L \rho A(\zeta) (R + \zeta) d\zeta \quad (8)$$

$$f_c(x) = \Omega^2 \left[ \int_x^{x_2^i} \rho A(\zeta) (R + \zeta) d\zeta + \sum_{j=i+1}^n \int_{x_1^j}^{x_2^j} \rho A(\zeta) (R + \zeta) d\zeta \right] \quad (9)$$

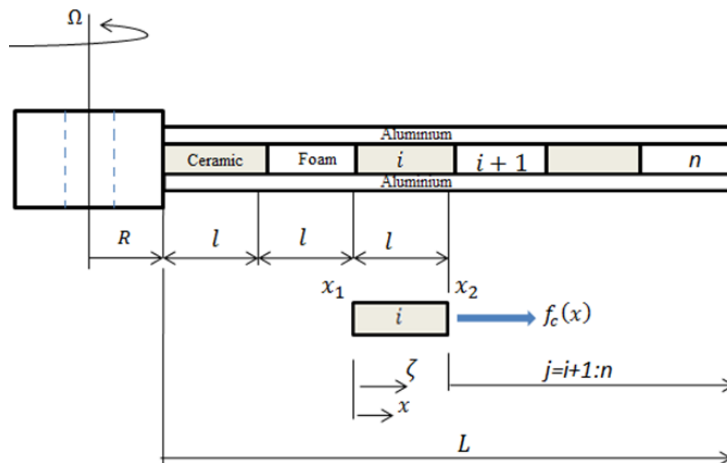


Fig. 2 Centrifugal force due to rotation

After making some mathematical manipulations, the centrifugal force can be cast in the form:

$$f_c(x) = f_o(x) + f_1(x) \quad (10)$$

where:

$$f_o(x) = -\Omega^2 [\rho_i A_i (Rx + 0.5 x^2)],$$

$$f_1(x) = \Omega^2 \left[ \rho_i A_i (Rx_2^i + 0.5 x_2^{i2}) + \sum_{j=i+1}^n \rho_j A_j \left( (Rx_2^j + 0.5 x_2^{j2}) - (Rx_1^j + 0.5 x_1^{j2}) \right) \right]$$

The same procedure introduced above can be applied to the blade subjected to torsion by replacing the term  $(\rho A)$  by mass moment of inertia about elastic axis  $(\rho I_0)$  in Eq. (10). Where,  $\rho_j A_j$  is average mass per unit length for the  $j^{th}$  element,  $\rho_i A_i$  is average mass per unit length for the  $i^{th}$  element, and R is hub radius

#### 4.2 Variational formulation of system energy

By taking the first variation of the first integral of an element total strain energy with ceramic core we get:

$$\begin{aligned} \delta U_{to}^p = & \int_0^L \delta(u_t') B1(u_t') + \delta(u_b') B2(u_b') + \delta(w'') B3(w'') + \delta(u_t') (B4)(u_b') \\ & + \delta(u_b') B4(u_t') + \delta(u_t') B5(w'') + \delta(w'') B5(u_t') \\ & + \delta(u_b') B6(w'') + \delta(w'') B6(u_b') + \delta(u_t) B7 \delta(u_t) \\ & + \delta(u_b) B7(u_b) + \delta(w') B8(w') - \delta(u_t) B9(u_b) \quad (11) \\ & - \delta(u_b) B9(u_t) - \delta(u_b) B10(w') - \delta(w') B10(u_b) \\ & + \delta(u_t) B10(w') + \delta(w') B10(u_t) \end{aligned}$$

By taking the first variation of the first integral of an element total strain energy with foam core we get:

$$\begin{aligned} \delta U_{to}^f = & \int_0^L \delta(u_t') C1(u_t') + \delta(u_b') C2(u_b') + \delta(w'') C3(w'') + \delta(u_t') (C4)(u_b') + \delta(u_b') C4(u_t') \\ & + \delta(u_t') C5(w'') + \delta(w'') C5(u_t') + \delta(u_b') C6(w'') + \delta(w'') C6(u_b') \\ & + \delta(u_t) C7 \delta(u_t) + \delta(u_b) C7(u_b) + \delta(w') C8(w') - \delta(u_t) C9(u_b) \quad (12) \\ & - \delta(u_b) C9(u_t) - \delta(u_b) C10(w') - \delta(w') C10(u_b) + \delta(u_t) C10(w') \\ & + \delta(w') C10(u_t) \end{aligned}$$

where B's by C's, are defined in (Badran *et al.* 2017).

By taking the first variation of the first integral of element strain energy due to rotation we get:

$$\delta U_R = \int_0^L \delta(w') f_c(x) (w') dx \quad (13)$$

By taking the first variation of the first integral of element total kinetic energy with ceramic core we get:

$$\begin{aligned} \delta T_{to}^p = \int_0^L & \delta(u_t)D1(u_t) + \delta(u_b)D2(u_b) + \delta(\dot{w}')D3(\dot{w}') + \delta(u_t)D4(u_b) \\ & + \delta(u_b)D4(u_t) + \delta(u_t)D5(\dot{w}') + \delta(\dot{w}')D5(u_t) + \delta(u_b)D6(\dot{w}') \\ & + \delta(\dot{w}')D6(u_b) + \delta(\dot{w})D7(\dot{w})dx \end{aligned} \quad (14)$$

By taking the first variation of the first integral of element total kinetic energy with foam core we get:

$$\begin{aligned} \delta T_{to}^f = \int_0^L & \delta(u_t)H1(u_t) + \delta(u_b)H2(u_b) + \delta(\dot{w}')H3(\dot{w}') + \\ & \delta(u_t)H4(u_b) + \delta(u_b)H4(u_t) + \delta(u_t)H5(\dot{w}') + \delta(\dot{w}')H5(u_t) + \delta(u_b)D6(\dot{w}') + \\ & \delta(\dot{w}')D6(u_b) + \delta(\dot{w})D7(\dot{w})dx \end{aligned} \quad (15)$$

where D's and H's are defined in (Badran *et al.* 2017).

By taking, the first variation of the total external work done on the element we get:

$$\delta W_t = \int_V \{\delta q\}^T \{f_b\} dV + \int_A \{\delta q\}^T \{f_s\} dA + \{\delta q\}^T \{f_p\} \quad (16)$$

Substituting Eqs. (11) - (16) in Eq. (1) we get the weak form of Hamilton's principle which we use in the finite element analysis.

## 5. Finite element formulation

The weak form of Hamilton' Principle stated in Eq. (1) will now be used to develop the finite element model of the suggested three-layer sandwich rotating blade with ceramic-foam core arranged side by side. Lagrange linear shape functions are used for axial displacement field  $u_t$ ,  $u_b$  which are  $C^0$ -type continuous, while Hermitian shape functions are used for transverse displacement  $w$ , which are  $C^1$ -type. This means that the deflection  $w$  and slope ( $\partial w/\partial x$ ) are continuous between two neighboring elements. The proposed model is a three-node finite beam element; each node has four mechanical degrees of freedom. The shape functions of the mechanical variables are similar to those in Badran (2018).

The element total stiffness matrix  $[K]$  will be derived with the help of Eqs. (11)-(12) for the different element with ceramic and foam cores after replacing the axial and transverse displacements by the assigned shape functions.

The stiffness matrix due to centrifugal acceleration can be derived using Eq. (13) as:

$$[K]_{c,f} = \int_{x_1^i}^{x_2^j} f_c(x) \delta_w^{eT} [N_w']^T [N_w'] \delta_w^e \quad (17)$$

where,  $[N_w']$  and  $\delta_w^e$  are the first derivative of transverse displacement and shape function respectively which are similar to those in Badran (2018).

The element total mass matrix  $[M]$  will be derived with the help of Eqs. (14) - (15) for ceramic and foam cores after replacing the axial and transverse displacements by the assigned shape functions.  $[K]$ ,  $[K]_{cf}$  and  $[M]$  are given in Badran (2018). Finally, the element nodal force

vector can be derived using Eq. (16).

By substituting the mass, stiffness and force vector in Eq. (1), the equation of motion of a finite element can be written as:

$$[M]\{\ddot{q}\} + \left[ [K] + [K]_{cf} \right] \{q\} = \{F\} \quad (18)$$

where, Coriolis effect are ignored, because the flexural and axial motion are uncoupled Banerjee and Kennedy (2014).

## 6. Periodic analysis

Periodic structures can be modelled like any ordinary structure, however, studying the behavior of one cell is sufficient to determine the stop and pass bands of the complete structure independent of the number of cells. In the present work, the frequency domain is classified into pass-bands, i.e. frequencies for which excited surface waves get through the periodic piezoelectric device, and stop-bands, i.e. frequencies which cannot pass through. Therefore, the piezoelectric device can be used for frequency filtering. There are two approaches for the analysis of the periodic characteristics of a beam: the forward approach and the reverse approach, as introduced in Badran (2008). A code was developed and validated for a periodic sandwich beam with a ceramic PZT (ignoring the piezoelectricity effect) and foam core, in order to study the effect of core structural periodicity on attenuating the vibration of beams.

## 7. Rotating blade flutter

The equations of motion are derived using energy methods by applying Hamilton's principle, which offers a convenient formulation for any number of discrete generalized or physical coordinates.

The assembled equation of motion of rotating blade has the form:

$$[M]\{\ddot{q}\} + [K]\{q\} = \{F\} \quad (19)$$

where,  $\{q\}$  is the coordinate vector containing both the twisting and bending degrees of freedom:

$$\{q\}^T = \{w_1 \quad \theta_1 \quad \varphi_1 \dots \dots \cdot w_N \quad \theta_N \quad \varphi_N\}^T$$

For flutter analysis, a harmonic motion with oscillation frequency  $\omega$  is assumed, so the governing equation becomes:

$$(-\omega^2[M] + [K])\{\bar{q}\} = \{\bar{F}\} \quad (20)$$

where,  $\bar{q}$  is the amplitude of the deformation vector,  $\bar{F}$  is the amplitude of the load vector,  $[M]$  is the global mass matrix, and  $[K]$  is the global stiffness matrix. In Eq. (20) the right hand side is derived using an aerodynamic model, and the left hand side is derived using the structural model. The natural frequency ( $\omega$ ) occurs in a free vibration case where the system acts independent of the external forces.

### 7.1 Structural model

Double symmetry of the structure cross section leads to decoupling of the bending and torsional motions. The loss of cross sectional symmetry leads to a coupling effect between the bending and torsional motions due to an offset between the center of gravity and the shear center; a distance referred to as inertial eccentricity (Tanaka and Bercin 1997). The resulting equations of motion are inertially coupled, but elastically uncoupled.

The coupled elastic potential energy (U) is given as:

$$U = \frac{1}{2} EI \int_0^L (w'')^2 dy + \frac{1}{2} GJ \int_0^L (\varphi')^2 dy \quad (21)$$

The coupled kinetic energy (T) is given as:

$$T = \frac{1}{2} \int_{chord} (\dot{h})^2 dm \quad (22)$$

By referring to (Badran *et al.* 2017),  $h = -w - em \alpha$

Substituting (h) in Eq. (22) it can be shown that, Guertin (2012)

$$T = \frac{1}{2} (\mu) \int_0^L (\dot{w})^2 dx + \frac{1}{2} (2 S_\alpha) \int_0^L (\dot{w})(\dot{\theta}) dx + \frac{1}{2} (I_\alpha) \int_0^L (\dot{\theta})^2 dx \quad (23)$$

By calculating the potential and kinetic energies of the structural model and applying Hamilton's principle, then using finite elements having two-nodes and three degrees of freedom per node (torsion, transverse displacement and rotation), we get the system of equations representing an eigen value problem. Solving these equations, we get the natural frequencies and mode shapes due to bending and torsion.

### 7.2 Aerodynamic model

The Theodorsen 2-D thin airfoil theory will be used to evaluate the unsteady aerodynamic forces and moments per unit span  $L_i$  and  $M_i$  using thin aerofoil theory with a Theodorsen's lift deficiency function, (Bisplinghoff *et al.* 1996).

These can be cast in a matrix form as follows:

$$\begin{Bmatrix} L_i \\ M_i \end{Bmatrix} = \omega^2 \begin{bmatrix} L_{1i} & L_{2i} \\ M_{1i} & M_{2i} \end{bmatrix} \begin{Bmatrix} h_i \\ \alpha_i \end{Bmatrix} \quad (24)$$

where:

$$L_{1i} = \pi \rho b_i^2 [L_h^i], \quad L_{2i} = \pi \rho b_i^3 \left[ L_\alpha^i - L_h^i \left( a + \frac{1}{2} \right) \right],$$

$$M_{1i} = \pi \rho b_i^3 \left[ M_h^i - L_h^i \left( a + \frac{1}{2} \right) \right],$$

$$M_{2i} = \pi \rho b_i^4 \left[ M_\alpha^i - (L_\alpha^i + M_h^i) \left( a + \frac{1}{2} \right) + L_h^i \left( a + \frac{1}{2} \right)^2 \right],$$

$\rho$ : air density,  $b_i$ : semi-chord,  $h$ : amplitude of the vertical displacement,  $\alpha_i$ : amplitude of the twisting angle,  $L_h^i$ ,  $L_\alpha^i$ ,  $M_h^i$  and  $M_\alpha^i$  are aerodynamic lift and moment coefficients,

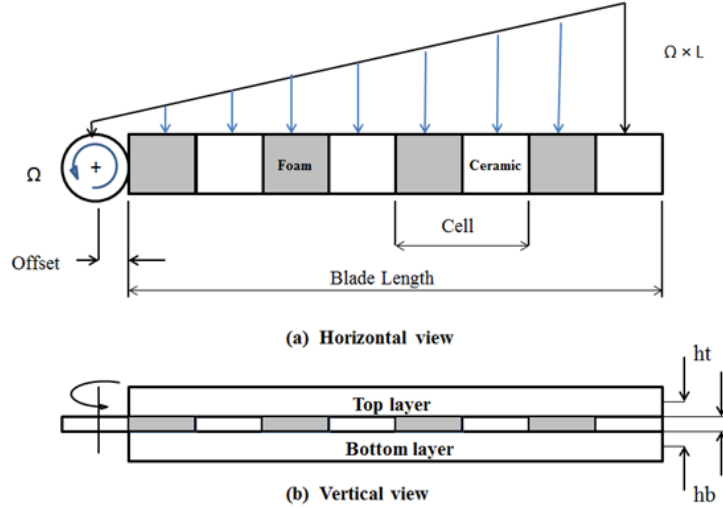


Fig. 3 Rotating periodic blade in hovering

$k_r$  : reduced frequency and can be assumed as  $k_r = \omega b_i/(\Omega L)$  for hovering and  $\omega$ : operating mode frequency as shown in Fig.3.

Also according to the chosen flight condition, the lift deficiency function will be determined, which depends on modelling the wake underneath the rotating blade. There are 3 different types of lift deficiency functions: (1) Theodorsen lift deficiency function originally developed for fixed-wing aircraft where flow is subjected to small disturbances. (2) Loewy's lift deficiency function assumed that the rotor blade sections will encounter the shed wake from previous blades in case of hovering. (3) Shipman and Wood's lift deficiency function, which is analogous to Theodorsen, and Loewy's, but was modified to account for the helicopter's forward speed and the build-up and decay functions associated with the advancing blade.

The external virtual work done by the aerodynamic forces per unit span at an aerodynamic node can be written as follows:

$$F_i = \Delta y_i \begin{bmatrix} \delta h_i & \delta \alpha_i \end{bmatrix} \begin{Bmatrix} L_i \\ M_i \end{Bmatrix} \quad (25)$$

Using three-node beam elements, the elastic axis deformation can be interpolated from the deformation of the two end nodes by using first order polynomials for the torsional twist angle and third order polynomials for the transverse displacement as follows:

$$u_e = \begin{Bmatrix} h_i \\ \alpha_i \end{Bmatrix} = [N]\{q\}_e \quad (26)$$

where  $[N]$ , is the shape function vector,  $\{q\}_e$  is the end nodes deformation vector in the wing local axes. Substituting Eq. (26) into Eq. (24) and then into Eq. (25) we get:

$$F_i = \omega^2 \{ \delta q \}_e^T [N]^T [L_i] [N]\{q\}_e \quad (27)$$

$$\text{where, } [\mathcal{L}_i] = \Delta y_i \begin{bmatrix} L_{1i} & L_{2i} \\ M_{1i} & M_{2i} \end{bmatrix}.$$

The elemental unsteady aerodynamic matrix  $[A]$  can be obtained by summing all the external virtual work done at all the aerodynamic nodes at the middle of the structural element (Badran *et al.* 2017) :

So, the equation of the dynamic system after assembling all matrices can be written as:

$$(-\omega^2[[M] + [A]] + [K])\{\bar{q}\} = 0 \quad (28)$$

The flutter analysis can be performed using the familiar  $V - g$  method (Bisplinghoff *et al.* 1996). The structural damping coefficient ( $g$ ) is introduced in the equations of motion, representing the amount of damping that must be added to the structure to attain neutral stability at the given velocity. Negative values of structural damping ( $g$ ) indicate that the structure is stable, while positive values indicate instability. Flutter occurs when the structural damping coefficient ( $g$ ) equals the actual damping of the structure, which is nearly zero, Hollowell and Dugundji (1984). Substituting in Eq. (28), the following eigenvalue problem is obtained:

$$\left( [K]^{-1} ([M] + [A]) - \left( \frac{1 + gi}{\omega^2} \right) [I] \right) \{\bar{q}\} = 0 \quad (29)$$

The above equation can be solved as:

$$([K]^{-1} [[M] + [A]]) \{\bar{q}\} = \left( \left( \frac{1 + gi}{\omega^2} \right) [I] \right) \{\bar{q}\} \quad (30)$$

$$([K]^{-1} [[M] + [A]]) \{\bar{q}\} = (Z[I])\{\bar{q}\} \quad (31)$$

The above equation can be solved for the complex eigenvalues ( $Z$ ) for several values of the reduced frequency by equating both the imaginary and real parts on both sides then we can calculate the flutter frequency ( $\omega_f$ ), damping ( $g$ ) and flutter rotation speed ( $\Omega_f$ ) as follows:

$$\omega_f = \sqrt{1/Z(Re)} , \quad \eta = Z(Im)/Z(Re) , \quad \Omega_f = \omega_f b/k_r \quad (32)$$

The values of ( $g$ ) and ( $\omega$ ) are plotted vs. ( $\Omega_f$ ), and the  $\omega$  value at  $g = 0$  represents the flutter frequency ( $\omega_f$ )

A MATLAB code was developed for the periodic rotating blade. The finite element model consists of two models: a structural model, which is a geometric model of the blade, and an aerodynamic model, which calculates the unsteady aerodynamic loads acting on the rotating blade. The UH-60's blade is modelled as a uniform beam, incorporating the average geometric and inertial characteristics of the blade. However, for the demonstration analysis the UH-60 blade will be modified to make it "flutter susceptible" by moving the chord-wise position of the blade c.g aft while keeping its elastic axis at the quarter chord. Physically, the method of solution in this work is equivalent to locking the blade at the 90-degree azimuth position and solving the flutter problems, similar to the fixed wing case with Theodorsen lift deficiency values. Allowing radial velocity, and thus, the reduced frequency, to vary with the span as in the case of the tangential velocity of a rotor blade in hovering.

A good agreement exists between the two sets of results giving confidence that the uniform

beam model is adequate as a first order approximation of a real blade (Badran *et al.* 2019).

### 8. The proposed periodic rotating blade model

We will choose the dimensions of the rotor under investigation so as to have the same aspect ratio of the UH-60 Black Hawk helicopter main rotor as follows Badran (2018) : Rotor radius = 6 m , Chord = 0.39 m , blade thickness = 10% chord , blade aspect ratio = 14.79. The properties of Aluminum are: Density  $\rho = 2770 \text{ Kg/m}^3$ , Modulus of Elasticity  $E = 71 \times 10^9 \text{ N/m}^2$  and Modulus of rigidity  $G = 27.3 \times 10^9 \text{ N/m}^2$ . The material properties of Ceramic PZT are:  $\rho = 7750 \text{ Kg/m}^3$ ,  $E = 70.8 \times 10^9 \text{ N/m}^2$  and  $G = 23 \times 10^9 \text{ N/m}^2$ . The material properties for Foam are:  $\rho = 75 \text{ Kg/m}^3$ ,  $E = 73 \times 10^6 \text{ N/m}^2$  and  $G = 26 \times 10^6 \text{ N/m}^2$ . The rotation speed  $\Omega = 20 \text{ rad/s}$ .

Now we study the effect of periodic design on the flutter hovering rotating speed of a helicopter rotor made of aluminum of three layers, top, core and bottom. In order to make a fair comparison between the solid and periodic core models we use the same outer dimensions, total mass, and flight conditions.

#### 8.1 The flutter speed of solid core rotating blade

It is that the flutter rotation speed of the solid core rotor is 26.6 rad/s, which is 1.32 times the reference rotation speed  $\Omega_0$  as shown in Fig. 4.

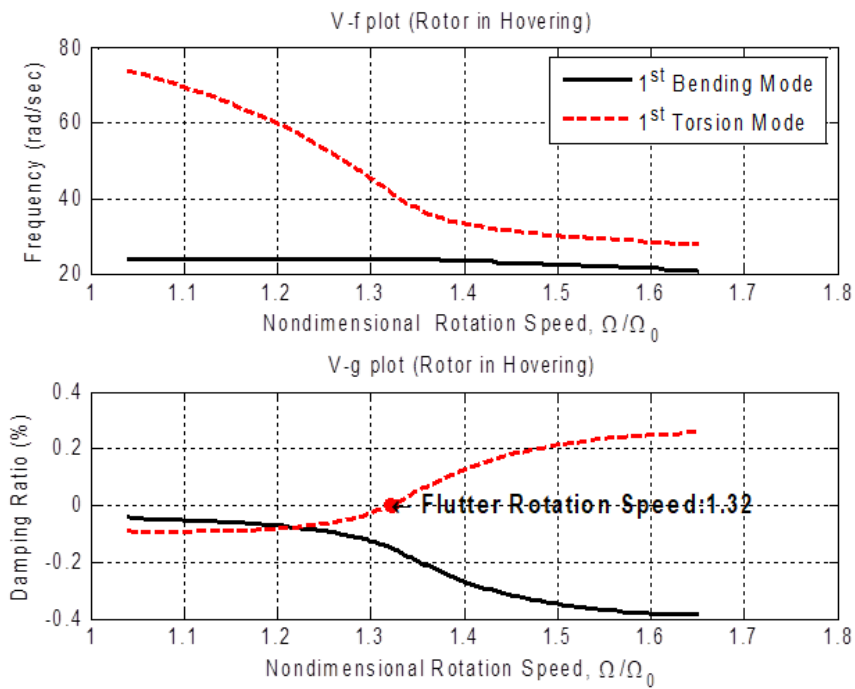


Fig. 4 Flutter rotation speed of the rotating solid blade

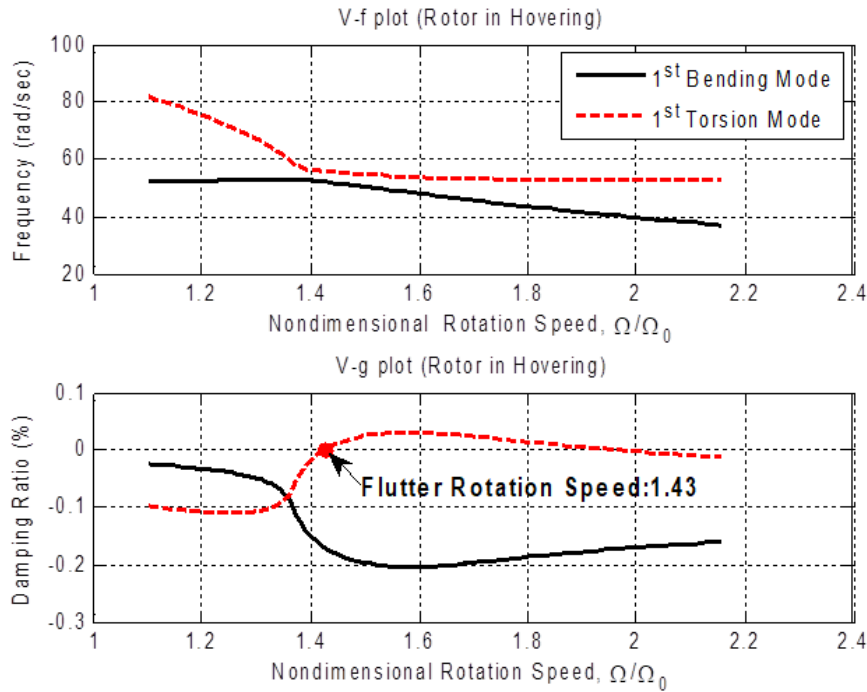


Fig. 5 Flutter rotation speed of the rotating periodic core blade in hovering (one cell)

Table 1 Variation of flutter frequency and flutter rotating speed with the number of cells

Rotor blade	Flutter frequency (rad/s)	Flutter rotational speed (rad/s)	Non-dimensional rotational speed ( $\Omega/\Omega_0$ )
Solid	41.57	26.44	1.32
Periodic (1 cell)	55.73	28.53	1.42
Periodic (2 cell)	229.49	149.41	7.47
Periodic (3 cell)	480.60	191.00	9.55
Periodic (4 cell)	816.20	286.72	14.33
Periodic (5 cell)	1267.50	356.02	17.80
Periodic (6 cell)	1271.30	345.89	17.29

## 8.2 Flutter speed of blade with periodic core

The proposed periodic core is a sandwich-rotating blade with three layers: the top and bottom layers are made of aluminum, and the core is periodic PZT Ceramic-Foam side by side. We choose the main geometry of the periodic model to be similar to that of the solid model, with the same total thickness and length. In this case the mass is 243.9 Kg for the solid rotor. So we will change the thickness of the layers to have a thickness ratio ( $h_p/h_t$ ) of 0.5 and the lengths of the cells to have a cell length ratio ( $L_p/L_t$ ) of 0.54. These values reduce the mass of the proposed periodic core model to that of the solid model.

Fig. 5 shows the flutter rotation speed of the proposed periodic core rotating blade at the same

altitude using one cell pair. The flutter angular speed of the sandwich periodic rotor is found to increase to 28.5 rad/s., which represent an improvement of 7%. This improvement can be explained by the existence of stop bands created by periodic design, which postpone the flutter frequency to a higher value.

Other calculations have been made to investigate the effect of increasing the number of cell pairs on the flutter forward speed of the rotor blade, keeping its outer dimensions, total mass, rotation speed and flight altitude unchanged.

Table 1 compares the frequency response of the solid rotor blade with that of the periodic blades having 3 and 6 cells pairs.

Table 1 gives the values of the flutter frequency and flutter rotor angular speed of the rotor blade for different numbers of cell pairs. It is seen from the results that great improvements in the flutter forward speed can be obtained by increasing the number of cell pairs in the periodic design of the rotor blade. The reason for large jumps in the flutter rotating speeds obtained for 2, 3 and 5 cells can be explained by the combined effect of the stop bands which shift the flutter frequencies to higher values, and the fact that higher modes of vibration become the ones which turn unstable. The improvement is found to diminish quickly after using 5 cells. Naturally, we should have used subsonic and supersonic aerodynamic theories when the blade tip speed increase to higher values. However, the obtained results using incompressible flow remain indicative of the flutter speed improvement by the use of periodic design.

## **9. Conclusions**

Aeroelastic performance of helicopter rotor blade structures is of extreme importance. A helicopter rotor blade must not experience flutter instability at all possible rotor speeds in hovering. Periodic design of structures has proved to be useful in improving the dynamic performance in the absence of flow. A periodic structure is composed of repeated groups of cells of different material or geometry. This causes destructive interference between the waves travelling back and forth along the structure, and hence reduces its vibration level.

In this paper a periodic rotor blade design is suggested as a rotating beam composed of a core sandwiched between two aluminium face layers. The beam is divided into cells in which the core is made of piezo ceramic or foam patches in an alternate order. The flutter rotation speed is calculated for such a periodic sandwich rotor using 3-node beam finite elements with shear, bending and torsional degree of freedom at each node in the structural analysis, and Theodorsen's 2-D thin aerofoil theory with a lift deficiency function for the unsteady aerodynamic analysis, assuming incompressible flow conditions. The blade flutter rotation speed is calculated using the V-g method for a different number of pairs of periodic cells, and compared with that of the non-periodic solid blade, keeping the outer dimensions, total mass (243.94 kg) and flight altitude (1000 m) unchanged.

Results of the calculations show that good improvements in the flutter rotation speed of the rotating blade can be obtained by using periodic design and increasing the number of periodic cells. This can be explained by the existence of the frequency stop bands created by the periodic design, which shift the flutter frequencies to higher values.

Also large jumps in the flutter rotation speed are observed at certain numbers of cells pairs. This is caused by the fact that higher modes of blade vibration become the ones which turn unstable. Finally, the improvement is found to diminish after using a certain number of cells.

## References

- Babu Gunda, J. and Ganguli, R. (2008), "New rational interpolation functions for finite element analysis of rotating beams", *Int. J. Mech. Sci.*, **50**(3), 578-588. <https://doi.org/10.1016/j.ijmecsci.2007.07.014>.
- Badran, H.T. (2008), "Vibration attenuation of periodic sandwich beams", M.Sc. Dissertation, Cairo University, Cairo, Egypt.
- Badran, H.T. (2018), "Improving dynamic and aeroelastic performance of helicopter rotors using periodic design and piezo active control", Ph.D. Dissertation, Cairo University, Cairo.
- Badran, H.T., Tawfik, M. and Negm, H.M. (2017), "Improving wing aeroelastic characteristics using periodic design", *Adv. Aircraft Spacecraft Sci.*, **4**(4), 353-369. <https://doi.org/10.12989/aas.2017.4.4.353>.
- Badran, H.T., Tawfik, M. and Negm, H.M. (2019), "Improving aeroelastic characteristics of helicopter rotor blades in forward flight", *Adv. Aircraft Spacecraft Sci.*, **6**(1), 31-49. <http://doi.org/10.12989/aas.2019.6.1.031>.
- Banerjee, J. and Kennedy, D. (2014), "Dynamic stiffness method for inplane free vibration of rotating beams including Coriolis effects", *J. Sound Vib.*, **333**(26), 7299-7312. <https://doi.org/10.1016/j.jsv.2014.08.019>.
- Bisplinghoff, R., Ashley, H. and Halfman, R. (1996), *Aeroelasticity*, Dover Publication Inc., Mineola, New York, U.S.A.
- Dayhoum, A., Zakaria, M.Y. and E. Abdelhamid, O. (2020), "Elastic torsion effects on helicopter rotor loading in forward flight", *Proceedings of the AIAA Scitech 2020 Forum*, Florida, Orlando, U.S.A., January.
- Filippi, M. and Carrera, E. (2015), "Flutter analysis of fixed and rotary wings through a one-dimensional unified formulation", *Compos. Struct.*, **133**, 381-389. <https://doi.org/10.1016/j.compstruct.2015.07.103>.
- Guertin, M. (2012), "The application of finite element Methods to Aeroelastic Lifting Surface Flutter", M.S. Dissertation, Rice University, Houston, Texas, U.S.A.
- Hammond, C.E. (1969), "Compressibility effects in helicopter rotor blade flutter", Ph.D. Dissertation, Georgia Institute of Technology, Atlanta, U.S.A.
- Hollowell, S.J. and Dugundji, J. (1984), "Aeroelastic flutter and divergence of stiffness coupled, graphite/epoxy cantilevered plates", *J. Aircraft*, **21**(1), 69-76. <https://doi.org/10.2514/3.48224>.
- Jones, W.P. and Rao, B.M. (1970), "Compressibility effects on oscillating rotor blades in hovering flight" *AIAA Journal* **8**(2): 321-329 DOI: <https://doi.org/10.2514/3.5663>.
- Kee, Y.J. and Shin, S.J. (2015), "Structural dynamic modeling for rotating blades using three dimensional finite elements", *J. Mech. Sci. Technol.*, **29**(4), 1607-1618. <https://doi.org/10.1007/s12206-015-0332-6>.
- Lim, I.G. and Lee, I. (2009), "Aeroelastic analysis of bearingless rotors with a composite flexbeam", *Compos. Struct.*, **88**(4), 570-578. <https://doi.org/10.1016/j.compstruct.2008.06.007>.
- Loewy, R.G. (1957), "A two-dimensional approximation to the unsteady aerodynamics of rotary wings", *J. Aeronaut. Sci.*, **24**(2), 81-92. <https://doi.org/10.2514/8.3777>.
- Mead, D. (1996), "Wave propagation in continuous periodic structures: research contributions from Southampton, 1964-1995", *J. Sound Vib.*, **190**(3), 495-524. <https://doi.org/10.1006/jsvi.1996.0076>.
- Mead, D. and Parthan, S. (1979), "Free wave propagation in two-dimensional periodic plates", *J. Sound Vib.*, **64**(3), 325-348. [https://doi.org/10.1016/0022-460X\(79\)90581-9](https://doi.org/10.1016/0022-460X(79)90581-9).
- Nitzsche, F., D'Assunção, D. and De Marqui Junior, C. (2015), "Aeroelastic control of non-rotating and rotating wings using the dynamic stiffness modulation principle via piezoelectric actuators", *J. Intell. Mater. Syst. Struct.*, **26**(13), 1656-1668. <https://doi.org/10.1177/1045389X15572011>.
- Reddy, J.N. (2002), *Energy Principles and Variational Methods in Applied Mechanics*, John Wiley and Sons, New York, U.S.A.
- Tanaka, M. and Bercin, A. (1997), "Finite element modelling of the coupled bending and torsional free vibration of uniform beams with an arbitrary cross-section", *Appl. Math. Modell.*, **21**(6), 339-344. [https://doi.org/10.1016/S0307-904X\(97\)00030-9](https://doi.org/10.1016/S0307-904X(97)00030-9).
- Theodorsen, T. (1935), "General theory of aerodynamic instability and the mechanism of flutter", NACA-

TR-496;Advisory Committee for Aeronautics, Langley, Virginia, U.S.A.

Yardimoglu, B. (2010), “A novel finite element model for vibration analysis of rotating tapered Timoshenko beam of equal strength”, *Fin. Elem. Anal. Des.*, **46**(10), 838-842.  
<https://doi.org/10.1016/j.finel.2010.05.003>.

Zhou, C., Lainé, J., Ichchou, M. and Zine, A. (2015), “Wave finite element method based on reduced model for one-dimensional periodic structures”, *Int. J. Appl. Mech.*, **7**(2), 1550018.  
<https://doi.org/10.1142/S1758825115500180>.

*AP*